A Composite Cycle Engine Concept with Hecto-Pressure Ratio

Sascha Kaiser*, Arne Seitz
Bauhaus Luftfahrt e.V., Munich, 85521, Germany

Stefan Donnerhack
MTU Aero Engines AG, Munich, 80995, Germany

and

Anders Lundbladh
GKN Aerospace Sweden, Trollhättan, SE-46181, Sweden

This paper describes research carried out in the European Commission funded Framework 7 project LEMCOTEC (Low Emission Core Engine Technologies). The task involved significant increase in core engine efficiency by raising the overall engine pressure ratio to over 100 (*hecto-pressure ratio*) by means of discontinuous cycles allowing for closed volume combustion. To this end, piston engines enable isochoric combustion and augment the conventional Joule/Brayton-cycle, thereby producing a *composite cycle*. An engine concept was chosen based on idealized parametric studies of simplified representations of the cycle as well as qualitative measures embracing weight, size, efficiency, emissions, operational behavior and the life cycle. The most beneficial mechanical representation of the Composite Cycle Engine in this study features crankshaft equipped piston engines driving separate piston compressors, a high pressure turbine driving an axial intermediate pressure turbo compressor, and a low pressure turbine driving the fan. The power plant performance calculations showed radical improvements in thrust specific fuel consumption of 17.5% during cruise. Although engine weight increases correspondingly by 31%, at aircraft level, a fuel burn reduction of 15.2% could be shown for regional operations relative to year 2025 engine technology. The concept is capable of meeting the emission reduction targets for CO_2 and NO_x aspired to by the LEMCOTEC project and the Strategic Research and Innovation Agenda (SRIA) targets for CO_2 in 2035, and for NO_x in 2050.

Nomenclature

Combined Cycle Engine – A sequential assembly of two independent heat engines, where the exhaust heat of the first cycle is being utilized as a heat source for the second cycle.
Composite Cycle Engine – An integrated assembly of at least two heat engine cycles featuring independent compression, heat source and expansion operating on the same working fluid.
Compound Engine – An engine that uses at least two different principles of power extraction that contribute to the output power working on the same working fluid, e.g. a turbine and a piston engine.

Symbols

BSFC	=	Brake Specific Fuel Consumption [lb/eshp-hr]
CPR	=	Charging Pressure Ratio [-]
EINOx	=	Emission Index NO_x [g_{NOx}/kg_{fuel}]
eshp	=	Equivalent shaft horse power, including effect of exhaust thrust [hp]
far	=	Fuel-Air-Ratio [-]

*Advanced Motive Power, Visionary Aircraft Concepts, Bauhaus Luftfahrt e.V, Willy-Messerschmitt-Str. 1, 85521 Ottobrunn, Germany

k	=	Reaction parameters [m^3/mol.s]
m	=	Mass [kg]
$\dot{m}$	=	Mass flow [kg/s]
M	=	Mach number [-]
n	=	Stage Count [-]
OPR	=	Overall Pressure Ratio [-]
p	=	Total pressure [Pa]
PAX	=	Nominal Seating Capacity [-]
PPR	=	Peak Pressure Ratio [-]
s_{NOx}	=	NO_x severity parameter [g_{NOx}/kg_{fuel}]
T	=	Total temperature [K], or thrust [N]
TSFC	=	Thrust Specific Fuel Consumption [g/kN/s]
war	=	Water-Air-Ratio [-]
φ	=	Crank shaft angle [rad]

Acronyms

ATAG	=	Air Transport Action Group
BPR	=	Bypass Ratio
CCE	=	Composite Cycle Engine
CR	=	Cruise
EIS	=	Entry Into Service
EoR	=	End of Runway
EU	=	European Union
FL	=	Flight Level
HPC	=	High Pressure Compressor
HPT	=	High Pressure Turbine
IATA	=	International Air Transport Association
IFSD	=	In-Flight Shutdown
IPC	=	Intermediate Pressure Compressor
ISA	=	International Standard Atmosphere
LDI	=	Lean Direct Injection
LEMCOTEC	=	Low Emission Core Engine Technologies
LPT	=	Low Pressure Turbine
MCL	=	Maximum Climb
NASA	=	National Aeronautics and Space Administration
NO_x	=	Nitrogen Oxides (nitric oxide for x=1, nitrogen dioxide for x=2)
PGB	=	Power Gearbox
PT	=	Power Turbine
RTF	=	Regional Turbofan
SL	=	Sea Level
SRIA	=	Strategic Research and Innovation Agenda
T	=	Core Turbine
TC	=	Turbo Compressor
TO	=	Takeoff
TOC	=	Top of Climb
TRL	=	Technical Readiness Level

I. Introduction

THE improvement of core engine efficiency is a major development target in order to reach emission reduction targets such as motivated by the European Commission's Flighpath 2050[1] and specified by the Strategic Research and Innovation Agenda (SRIA)[2], or by IATA and ATAG[3], or by NASA[4], and to improve operating economics of civil aircraft. Increasing the Overall Pressure Ratio (OPR) of an ideal Joule/Brayton-cycle with ideal gas generally results in an increase of engine efficiency. However, this rule does not hold for extreme OPRs when assuming non-ideal components, i.e. component efficiencies below unity, or real gas. In reality, however, material limits and clearance losses restrict the OPR. Increasing OPR results in an increase of the High Pressure Compressor (HPC) exit temperature, affecting HPC and combustion chamber material choices. The turbine cooling air temperature also increases with OPR, requiring higher amounts of cooling air for a given permissible turbine material temperature. In addition, the flow path cross sections of the last HPC stages decrease with increasing OPR. This results in shorter blades and higher tip losses. Therefore, an optimum OPR exists for the conventional Joule/Brayton-cycle depending on material temperature limits and component efficiencies[5], and an increase in OPR beyond this point does not yield improved engine efficiency. The engine with the highest OPR currently in service is the GEnx-1B76 with an OPR of 58 at top-of-climb. In the LEMCOTEC project, engines with an OPR up to 70 are being investigated.

To this end, a fundamental change of the underlying thermodynamic cycle is warranted to allow for a significant further improvement of aeronautical engine efficiency. Discontinuous cycles provide the advantage of temporary exposure to extreme temperatures and pressures to the material and, thus, allow for reaching pressure ratios over 100, i.e. hecto-pressure ratio. The Seiliger cycle - the idealized representation of the thermodynamic cycle in piston engines – is expected to have the highest potential for the implementation of discontinuous cycles into a real engine due to its technical maturity.

Piston engines had been the prevailing class of aero engines until the mid-1950s and are still predominant in the land-based and marine transport sectors. As shown in Table 1, so-called *compound engines* had a Brake Specific Fuel Consumption (BSFC) in takeoff (TO) comparable to the most recent large turboprop engines[6]. Compound engines use at least two different principles of power extraction contributing to the output power working on one fluid[7]. Typically, a compound engine is composed of a piston engine providing the greater share of the output shaft power and a turbine supporting the piston engine. Although these engines were designed and manufactured in the 1950s, they already featured peak pressures of up to 14MPa (2000psi) and peak temperatures up to 2800K[8]. Consequently, they already achieved hecto-pressure ratios and exceeded peak pressures and temperatures indicative of contemporary turbo engines.

Table 1. Performance characteristics of compound engines and turboprop engines.

Compound engines	**BSFC [lb_m/eshp-hr] at TO SL**	**Power-to-Weight ratio [eshp/lb_m]**
Wright R-3350 (1941)[9]	0.38	0.82
Napier Nomad E.145 (1954)[8]	0.35	0.88
Turboprop engines		
Allison T-56 (1955)[9]	0.52	2.43
Rolls-Royce AE 2100 (1994)[10]	0.41	2.76
Europrop TP400 (2009)[10]	(cruise) 0.35	2.68

The downside of these engines was their weight, about three times higher than that of turboprop engines for given power (cf. Table 1). In these compound engines, the piston engine provided the main share of shaft power in the basic design, and the turbo components only provided limited output power. This design paradigm inherently resulted in large piston systems and high engine weight. In turn, this limited maximum cruise speed and altitude. Uncharged piston powered aircraft were, therefore, not even able to fly above the weather. Moreover, the compound engines were highly complex, having many accessory shafts and gears. The concept introduced in this paper will address these disadvantages of compound and piston engines. The presented approach utilizes the excellent performance characteristics of piston engines whilst utilizing the excellent power-to-weight ratio of turbo components where applicable. Accordingly, the transition between stationary turbo component flow and pulsating piston engine flow needs to moderated with additional means, such as buffering volumes, and turbo component performance may be impaired. Further challenges of piston engines were associated with In-Flight Shutdown (IFSD) rates that were about ten times higher than that of contemporary ETOPS 180 min certified aircraft[11,12]. With tremendous improvements in production techniques and tolerances in the automotive industry, as well as engineering materials over the past decades, the reliability of piston based aeronautical engines can be expected to allow for robust operation close to modern turbofan reliability. Finally, the relatively low fuel price at the time lead to an understatement of fuel efficient engines. In contrast, engine efficiency has gained a lot of importance today since fuel price constitutes a large share of the direct operating costs of an aircraft[13] and due to emission reduction targets mentioned before.

The presented *Composite Cycle Engine* (CCE) concept defines an integrated assembly of at least two heat engine cycles featuring independent compression, heat source and expansion. The term was originally used to advertise the

Napier Nomad E.125 engine for its innovative combination of diesel engine and gas turbine[14]. The term *composite cycle* should be distinguished from the established term *combined cycle*. The latter refers to machines with a sequential arrangement of heat engine cycles with the exhaust heat of the first cycle being utilized as a heat source for the second cycle (this arrangement is typically used as a gas turbine providing its exhaust heat for a steam turbine)[15]. The thermodynamics of the composite cycle is schematically shown in Figure 1(right) with a piston engine driving a piston compressor. It is based on the idea of the topping cycle. The bottom cycle is composed of heat addition by the combustion chamber, and a turbine driving a turbo compressor. Considering the compression potential of piston machines, CCEs are seen to be an appropriate enabler for hecto-pressure ratio cores. The handling of technical challenges concerning instationary flow by piston component and material requirements is addressed in the engine design (Section IV). Due to special circumstances at combustion with high temperatures and pressures, NO_x emissions are assessed with a dedicated model for the piston system and for the combustion of vitiated air.

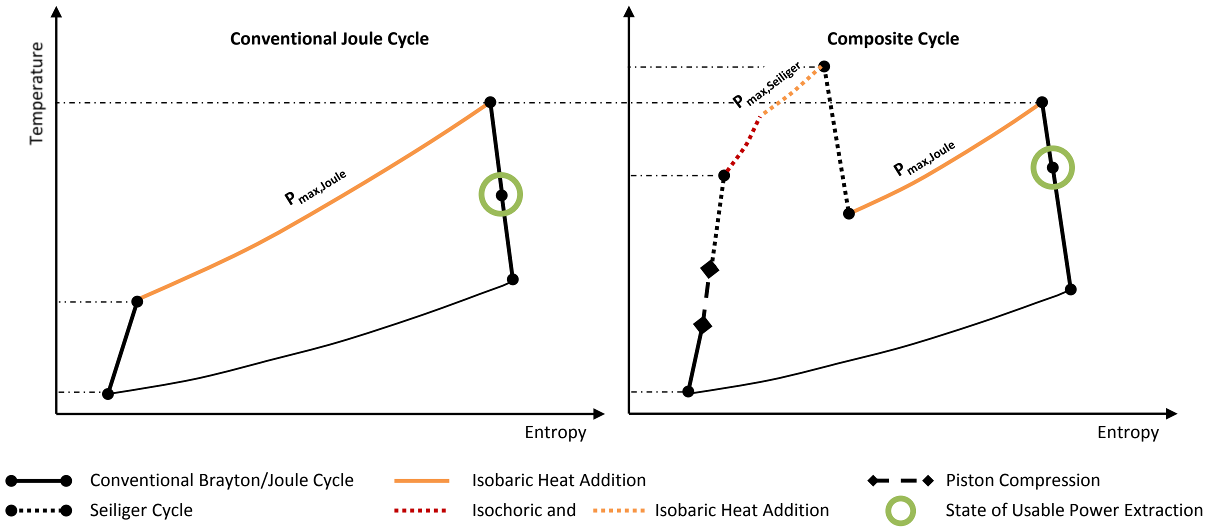

Figure 1. Schematic illustration of a Joule/Brayton-cycle (left) and a composite cycle (right).

Other options to modify the cycle include intercooling to mitigate material constraints[16,17]. These have been omitted in the scope of this paper in order to limit engine complexity. Nonetheless, intercooling may synergize very well with the composite cycle engine concept. When intercooling is applied in front of the piston engine, its size and, hence, its weight penalty could be reduced in addition to the thermodynamic benefits of intercooling.

The presented CCE concept was investigated in the LEMCOTEC project Work Package “Future Cycle Studies” targeting concepts for an Entry Into Service year range of 2030 to 2050. The improvement potential of the CCE concept is evaluated in contrast to a generically defined Regional Turbofan (RTF) reference engine with an expected technology standard of year 2025[18]. The RTF is a two spool geared turbofan with a maximum OPR of 50. The application case is a large regional aircraft platform (design range 2000nm; 100 PAX; maximum TO weight 50 200kg = 110 700lb_m; M0.78; EIS 2000).

II. Selection of the Concept Architecture

The efficiency of the piston engine originates from the discontinuous mode of operation. First, this allows for much higher combustion temperatures since the material is exposed to these only for very short times of the order of milliseconds. Second, this enables closed volume combustion that features partially isochoric (constant volume) combustion. Heat addition in a constant volume results in pressure rise. In contrast to the Joule/Brayton cycles, this additional compression does not need to be driven with shaft power, inherently resulting in higher engine efficiency. Another advantage of closed volume processes is the increased compression and expansion efficiencies because typical turbomachinery losses, especially tip losses, are lower or even not present.

In order to address the drawbacks of former compound engines, three design paradigms have been formulated for the presented CCE concept:

1. A power turbine is designed to deliver a substantial amount of usable shaft power. A major challenge associated with integrating piston engines is connected to the unfavourable power-to-weight ratio of large piston engines. Here, previous concepts used the piston engine for shaft power delivery and the turbo-

components primarily as a charging device. This paradigm avoids large piston system dimensions and utilizes the outstanding power-to-weight ratio of turbines.

2. A turbo compressor must be implemented in front of the piston system. A substantial charging of the piston system may be achieved in this manner to reduce piston size and weight.
3. The piston system may consist at least of a piston engine featuring combustion. A piston system may consist of *piston engines* featuring a combustion process in the cylinder and *piston compressors*, only compressing air without combustion taking place. Although the superior piston compressor efficiency could be utilized with a piston compressor only, the main advantages of closed volume combustion would not be achieved.

The resulting fundamental architecture is depicted in Figure 2. The piston system only operates in the core of the engine where the pressures and temperatures are highest. The remainder of the engine constitutes a conventional turbo engine set up with a fan driven by a Power Turbine (PT), and an Intermediate Pressure Compressor (IPC) driven by a High Pressure Turbine (HPT) charging the piston core. The piston system is followed by a conventional combustion chamber. The pressure characteristics are depicted schematically indicating the pressurized combustion and the pre-compression driven by the piston engine. The high-pressure core of the gas turbine is replaced by a generic piston system that serves as placeholder for concept ideas.

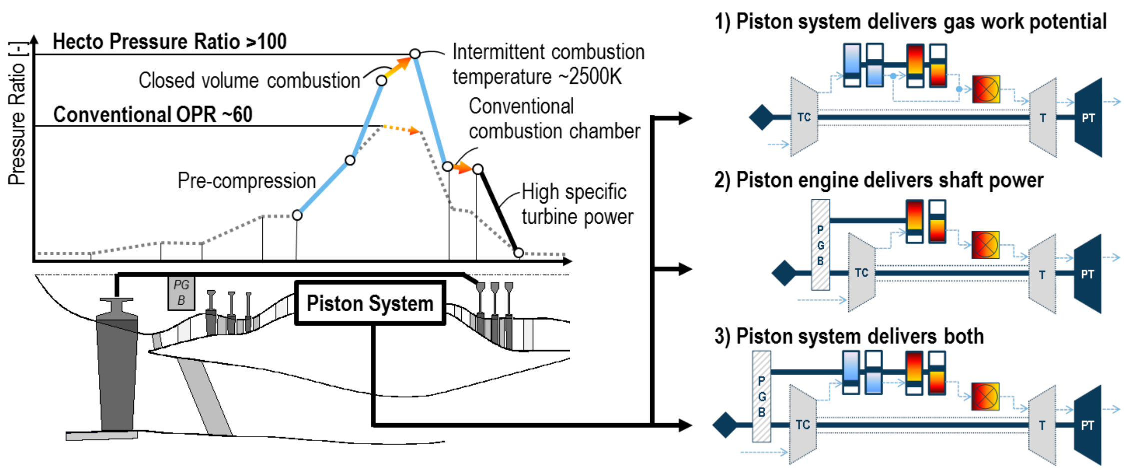

Figure 2. Schematic illustration of the composite cycle engine. The piston system may comprise concept dependent numbers of piston compressors (blue pistons) and piston engines (orange-red pistons). The acronyms denote: PGB – Power GearBox, TC – Turbo Compressor, T – core Turbine, PT – Power Turbine.

Three fundamental working principles have been derived and are depicted in Figure 2 (above, right). In the first concept, all excess power of the piston engine is used to drive a (piston) compressor. The integrated piston system converts fluid to a state of higher work potential, which allows the extraction of shaft power. In the second concept, all excess power of the piston engine is delivered directly to the output shaft. The third concept is a combination of both.

First, the identified architectures were analyzed with a simplified thermodynamic model for concept selection. The thermodynamic model was built based upon polytropic efficiencies for compression and expansion, combustion efficiency, ideal gas, and fixed power-to-weight ratios for turbo and piston components for weight estimation. The maximum permissible temperatures were assumed to be 1900K in the combustion chamber and 2300K in the piston engine. Although temperatures in modern piston engines may reach up to 2900K[19], the maximum permissible temperature was restricted to cope with the high inlet temperatures and, thus, high mean temperatures in the piston. Subsequently, the cycle characteristics were evaluated based on specific work, thermal efficiency, and weight of the core engine. Additionally, qualitative criteria pertaining to efficiency, geometry, weight, emissions, operational behavior, and life cycle were assessed.

Thermodynamic studies showed that a design point with Charging Pressure Ratio (CPR) of 54 provides greatest improvement in thermal efficiency while limiting peak pressure and weight increase. The peak pressure ratio was restricted to 325 at maximum climb, to avoid absolute peak pressures in excess of 25MPa (3 600psi)[20] during takeoff. The attainable improvement in thermal core efficiency is about 20% points compared to a reference Joule/Brayton-cycle with a pressure ratio of 60. The specific power by the cycle is up to 90% higher, while the mass increases by about 20%. Even though Concepts 2 and 3 exhibit slightly higher potentials for utilization of piston efficiency and specific work, the expected weight increase is higher and the part power behavior expected to be worse. The first concept (where the piston system delivers fluid work potential only) was found to provide the greatest overall benefits. Main advantages of this concept are low geometric restrictions, lower mechanical loads, and an additional operational degree of freedom due to the missing mechanical connection to the low pressure spool. It is further elaborated below. All concepts have also been examined without the Joule/Brayton combustion chamber, but were less favorable due to a large increase in engine size and weight, as well as thermal load on the piston system. The missing degree of freedom of the second heat addition represents a further major drawback of omitting the Joule/Brayton combustion chamber.

For the conceptualization of the chosen architecture, it was decided to aspire to a concept that features a sufficiently high technical maturity and potential for realization, i.e. components with the highest possible Technical Readiness Level (TRL). An initial elaboration of the chosen concept is depicted in Figure 3. The HPT drives a radial IPC and the Low Pressure Turbine (LPT) drives the propulsor only. The choice for a radial IPC was motivated by reduced component size and weight, as well as improved spatial arrangement. The piston system is implemented as a multiple V-type piston layout driven by 2-stroke diesel engines. A crankshaft connects piston engine cylinders and corresponding piston compressor cylinders. The piston systems are wrapped around the core turbo engine as conceptually visualized in the cross-sectional view in Figure 3 (right). Buffering volumes moderate flow fluctuations between the discontinuously operating piston system and the quasi-stationary turbo components in order to reduce pulsation within IPC exit and HPT inlet conditions.

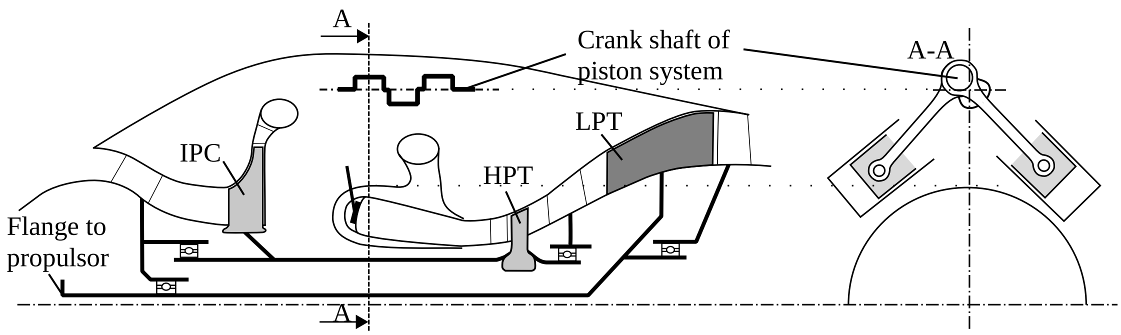

Figure 3. Conceptual Sketch of the chosen CCE illustrating possible mechanical representations of the thermodynamic cycle.

III. Design and Analysis Methods

CCE performance and size were determined using an in-house integrated engine simulation environment, which allows to incorporate effects from component matching, to provide a more realistic representation of the piston process, and to produce off-design characteristics (part load behavior and differing operating conditions). This is important for the assessment of thrust capabilities in important sizing points, especially during takeoff (TO) and at top of climb (TOC). The simulation environment was verified against the well-known gas turbine performance software GasTurb®[21] for its methods and integrated functionality. The off-design behavior of turbo components was modelled with scaled, generic component maps[22] for the inner and outer fan, the IPC, the HPT and the LPT. The component efficiencies were set to be equal to the reference engine. Expected technological improvements were assumed to be diminished by reduced turbo component size and impairment due to pulsating flow imposed by the piston engine. Thermodynamic properties of air are obtained through interpolation in tabulated data for mixtures of air, fuel-air-ratio (far) and water-air-ratio (war)[23].

The piston engines and piston compressor were modelled as 1D perfect mixing control volumes[24]. The thermodynamic state of the fluid in the piston is represented as one (mean) value only and is only resolved in the time domain, and corresponding crank shaft angle φ. The program has been validated against crankshaft resolved data from a two-stroke engine simulation program[25].

A method for predicting CCE NO_x emissions has been developed for both the piston engine and the Joule/Brayton combustion chamber. For the piston engine, reaction kinetics are used to estimate NO_x creation based on time resolved data for temperature and pressure from the 1D piston model. The three major NO formation mechanisms are thermal NO, prompt NO, and fuel NO. Only thermal NO has been considered since it typically constitutes about 95% of the total NO_x formation in piston engines[26]. Thermal NO creation is simulated with the Zeldovich mechanism consisting of the following reactions:

$$O + N_2 \overset{k_1}{\leftrightarrow} NO + N \qquad \text{Reaction 1}$$
$$N + O_2 \overset{k_2}{\leftrightarrow} NO + O \qquad \text{Reaction 2}$$
$$N + OH \overset{k_3}{\leftrightarrow} NO + H \qquad \text{Reaction 3}$$

The reaction parameters k_i for the chemical reactions that determine the speed of the reaction are dependent on temperature and pressure, and are well examined for this set of reactions[27]. With the reaction rates, the change in the concentration of oxygen [O], nitrogen [N] and nitrogen oxide [NO] can be derived. The reaction rates from NO to NO_2 have been neglected since they have no impact on the combined NO_x emission rates. The Emission Index NO_x EINOx results from integration of the changes over an entire piston cycle.

Since inhomogeneity of the temperature in the piston is neglected in the 1D piston model, NO_x formation is underestimated. Therefore, a semi-empirical model based on measurements of automotive piston engines[28] was incorporated into the model to account for stoichiometric zones during combustion. According to this model, piston engines always produce a minimum emission of $17.5 g_{NOx}/kg_{fuel}$[28] in the zones of combustion, and, additionally, a component that is dependent on process parameters. As a result, the term that scales with the process parameters has been replaced with the emission index obtained from the reaction kinetics model:

$$\text{EINOx} = 17.5 + \text{EINOx}_{\text{reaction kinetics}} \qquad \text{Eq. 1}$$

Thus, the piston engine always has a minimum of NO_x emissions irrespective of the process parameters. The constant offset can be regarded as a technology factor. A reduction of the offset may be motivated by measures like stratified charge combustion and exhaust gas recirculation[29], but was not assumed in this paper.

The Joule/Brayton combustion chamber NO_x emissions were estimated based on the NO_x severity parameter s_{NOx}[21]:

$$s_{\text{NOx}} = \left(\frac{p_3}{2964.5\text{kPa}}\right)^{0.4} \cdot \exp\left(\frac{T_3^* - 826.26K}{194.39\text{K}} + \frac{6.29 - 100 \cdot \text{war}}{53.2}\right) \qquad \text{Eq. 2}$$

The combustion chamber entry pressure p_3 and temperature T_3 as well as the water-air ratio war have an impact on the NO_x formation. Due to the reduced oxygen availability after the piston engine, the stoichiometric flame temperature T_s reduces considerably by several hundred Kelvin. To this end, T_s was calculated first based on the chemical reaction of kerosene with the vitiated air[30]. Then, the equivalent combustion chamber entry temperature T_3^* that would yield identical T_s with fresh air was calculated. Finally, the emission index from the Joule/Brayton combustion chamber was obtained by scaling s_{NOx} by a factor of 20, which was derived for contemporary aircraft engines from the ICAO Aircraft Engine Emissions Databank[31]. With lean combustion technology such as Lean Direct Injection (LDI)[32], this factor may be further reduced slightly, although the Joule combustion chamber contributes the minor share to NO_x emissions. Potential reduction of NO_x concentrations in the Joule/Brayton combustion chamber due to back reaction were neglected, although experience from stationary gas turbines with sequential combustion suggests a significant impact due to the back reaction[33]. Another factor potentially reducing NO_x production in the Joule/Brayton combustion chamber originates in the potential for flameless combustion and lower residence times owing to the increased inlet temperature and, hence, better fuel evaporation as well as the presence of oxygen radicals from the first combustion fostering the chemical reactions[34].

The weight of the piston engine was estimated with a method based on simple geometric representations of the piston and the cylinder. The cylinder was conservatively assumed to have an average wall thickness of 8mm[35], and was assumed to be produced from nickel-based alloy for its superior mechanical properties at high temperatures[19]. The piston was represented with typical aspect ratios for important dimensions such as the compression height[36], and was assumed to be produced from aluminum-silicon alloy due to its low density while having a high temperature resistance[36]. The resulting piston weight with these assumptions is proportional to the third power of the piston diameter. Typical values of the proportionality constant for light-weight cylinders of about $0.4 g/cm^3$ have been determined[35]. The weight of connecting rod, crankshaft, flywheel, cylinder head, oil system and other accessories were assumed to be proportional to the sum of piston and cylinder weight. The scaling constant was derived from empirical values[37]. Consequently, the combined piston and cylinder weight was scaled by a factor of 2.6.

The weight of the CCE turbo components has been estimated based on the reference component weights. Fan weight and nacelle weight did not change since the fan diameter was kept constant. Other component masses m_i were scaled based on stage count n_{st} of the component and corrected mass flow $\dot{m}_{\text{corr}} = \frac{\dot{m} \cdot \sqrt{T}}{p}$ of the component inlet:

$$m_{i,CCE} = m_{i,RTF} \cdot \frac{n_{\text{st,CCE},i}}{n_{\text{st,RTF},i}} \cdot \frac{\dot{m}_{\text{CCE},i} \cdot \sqrt{T_{\text{CCE},i}} \cdot p_{\text{RTF},i}}{\dot{m}_{\text{RTF},i} \cdot \sqrt{T_{\text{RTF},i}} \cdot p_{\text{CCE},i}} \qquad \text{Eq. 3}$$

The component inlet conditions are specified with the corresponding mass flow $\dot{m}$, the total temperature T and the total pressure p. The formula was evaluated assuming typical Maximum Climb (MCL) rating at Top of Climb (TOC), representing the turbo component sizing conditions. Shaft weight was scaled linearly with engine length. Other weights including casings, buyer furnished equipment, fluids, and mounts were assumed to be constant. Accessory weights are assumed to reduce by 50kg due to simplified engine startup capabilities by virtue of the piston engine.

Fuel burn was assessed with exchange factors for a year 2000 reference aircraft platform for isolated changes in Thrust Specific Fuel Consumption (TSFC), weight, and fan diameter given in Table 3 (p. 11). These exchange factors state the fuel burn saving sensitivities for a resized aircraft utilizing all cascading effects.

IV. Engine Design and Performance

The CCE design point was optimized for a high improvement in TSFC while respecting temperature limits for a maximum permissible Joule/Brayton combustion chamber inlet temperature of 1250K and a maximum piston engine exhaust temperature of 1420K, which was extrapolated from former studies on compound engines[38]. An uncooled LPT was not achievable with the chosen setup, so that a low amount of cooling air needs to be provided for the LPT. The temperature limits are depicted in Figure 4. The chosen design point serves as a best and balanced compromise between improving TSFC and limiting piston system weight, with the focus on minimizing fuel burn. It is interesting to note that the TSFC of CCEs improves with decreasing combustor exit temperature T_4 contrary to conventional turbofan engines. This results from a shift of fuel from the Joule/Brayton combustion chamber to the highly efficient piston engine, which yields higher overall engine efficiency.

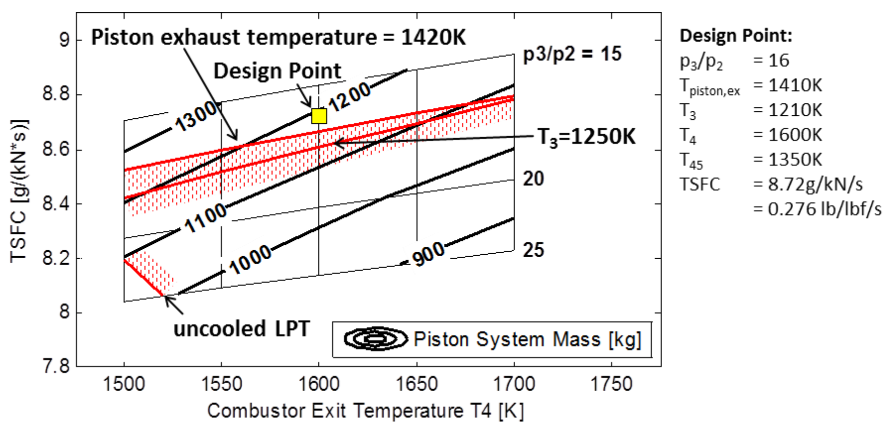

Figure 4. Parametric design point study altering combustor exit temperature T_4 and pressure ratio p_3/p_2 for takeoff conditions (SL, M0.25, T=66.1 kN).

The most important performance characteristics of the integrated engine performance calculation are presented in Table 2 (overleaf) for Sea Level (SL) End of Runway (EoR) conditions at $\Delta T_{\text{ISA}} = 15\text{K}$ and Top of Climb (TOC) conditions at $\Delta T_{\text{ISA}} = +10\text{K}$. The TSFC improves by 14.3% at takeoff and 18.2% at top of climb. Although the mass-averaged pressure ratio behind the piston compressor, denoted as Charging Pressure Ratio (CPR) is only 24.4 at TOC, the simulated Peak Pressure Ratio (PPR) reaches values of 324, which is close to the value expected in Section II and well beyond the aspired pressure ratio of 100. The exit temperature of the combustion chamber reduces to 1600K for optimum efficiency. Since heat addition in the piston engine is more efficient due to pressurized combustion.

For contemporary turbo machines, the aerodynamic design of the engine is performed for MCL rating at TOC since this is the critical sizing condition for turbo fan engines with very high Bypass Ratio (BPR) greater than 10, yielding maximum corrected mass flows[39]. CCEs require a mixed approach to component sizing, since the critical turbo component sizing condition is still MCL at TOC, while the piston system critical sizing condition is the piston peak pressure, which occurs during TO. It was limited to 25MPa (3 600psi)[20].

Table 2. CCE Performance parameter in contrast to the reference RTF.

	TO (SL, M0.25, T=66.1 kN)		MCL (FL350, M0.75, T=18.4 kN)	
Parameter	**RTF**	**CCE**	**RTF**	**CCE**
TSFC [g/s/kN]	10.17	8.72	15.44	12.63
TSFC Delta [%]	-	-14.3	-	-18.2
BPR [-]	12.1	17.4	11.0	15.2
CPR [-]	-	17.3	-	24.4
OPR / PPR [-]	38.8	237	50.0	324
T4 [K]	1900	1600	1810	1416

The resulting engine dimensions and component arrangement is shown in Figure 5. The piston system has a major impact on the core engine layout. The overall engine size, however, does not increase compared to the reference since the HPC was dispensed with, and the core flow is 28% lower compared to the reference. This is also reflected in the increase of bypass ratio in MCL from 11.0 to 15.2. The piston system does not impair the bypass ducting since it fits into the geometric boundaries of the core engine. The piston system is composed of 3 individually operating units and each consists of 4 piston engine cylinders driving 8 piston compressor cylinders. The cross-sectional view in Figure 5 (right) shows that the piston engines have a slightly smaller cylinder diameter of 0.18m (7.2in) than the piston compressors of 0.23m (8.9in). The piston compressor arrangement could be relaxed by staggering the cylinder banks, although this would increase the piston system length by half a cylinder.

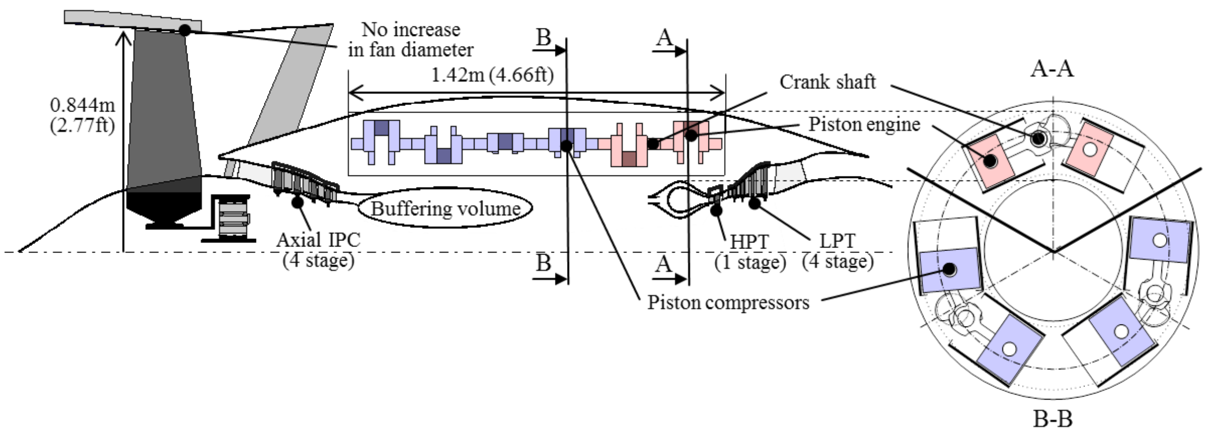

Figure 5. General arrangement of the CCE. The V-type piston systems are arranged circumferentially around the engine core (right).

The buffering volume indicated behind the IPC moderates between the IPC exit flow and the instationary piston compressor inlet flow. The volume is sized to reduce the pressure oscillations at the IPC exit to 0.2% of the total pressure to avoid performance losses and susceptibility to surge. At this amplitude, no negative impact on turbine efficiency is expected. As a sizing guideline, the buffering volume needs to have a size of 10 times the displacement volume ingested during a piston compressor cycle. The resulting volume of the buffer after the IPC is 0.089m^3 (3.14cu.ft). While the component indicated provides the entire volume, it may be smaller in reality since the ducts connecting IPC and piston system also contribute to the volume. The buffering volume connecting piston system exit and combustion chamber inlet has a size of 0.044m^3 (1.57ft^3) and is not shown in the drawing. Nevertheless, enough space is available for the buffer, and the combustion chamber serves as an additional buffer in front of the HPT.

The IPC provides a pressure ratio of 3.35 in MCL, which yields a moderate stage pressure ratio of 1.35 for a high speed compressor[39,40]. It is implemented as an axial compressor since the radial compressor with a lower efficiency leads to higher piston system weight and it does not improve component arrangement. The single stage HPT drives the IPC off a pressure ratio of 1.51 in MCL. The 4 stage LPT drives the fan only with a pressure ratio of 10.8 in MCL.

The part load curve of the CCE as depicted in Figure 6 (overleaf) shows that the CCE has an excellent efficiency characteristic during cruise, resulting in mean TSFC improvements for the design mission of 17.5% and even 18.5% on the 500nm mission. This is a result of the CCE characteristic that allows for reducing the fuel flow to the comparatively inefficient Joule/Brayton combustion chamber, while maintaining the power level of the piston engine combustion. As a result, the typical bucket curve characteristic of turbofan engines, resulting in a TSFC minimum in cruise, is considerably shifted towards lower thrust.

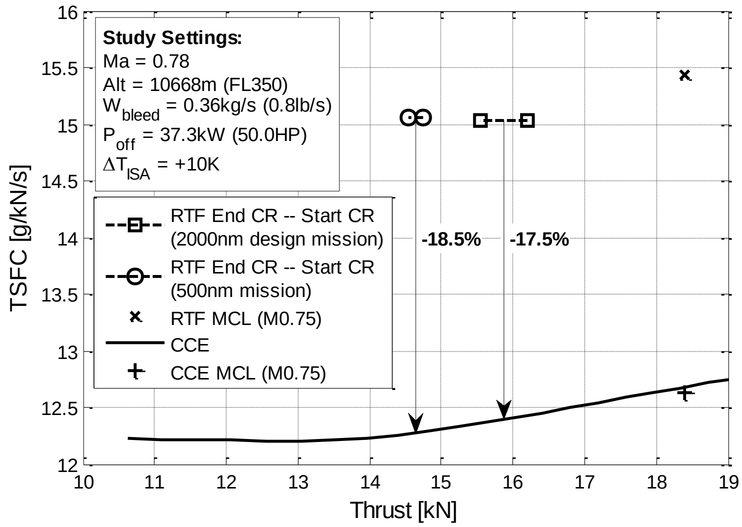

Figure 6. Thrust Specific Fuel Consumption v thrust of the CCE during cruise (CR) in contrast to the RTF.

The NO_x emissions of the CCE are at a low level of 19.8g/kN, and are 10% lower than to the RTF emissions with 22.0g/kN[41], which achieves very low NO_x emissions by means of an Lean Direct Injection (LDI)[32] combustor technology. Benchmarking the engine against the permissible emission according to ICAO Annex 16 CAEP/6[42] would yield a margin of -84%, assuming the reference pressure ratio of the CCE to be based on the time-averaged pressure in the piston engine. This would allow for meeting the SRIA targets for 2050[2] of -75% NO_x in the LTO cycle vs. CAEP/6, or the NASA N+3 goal of CAEP/6-75%[4]. The latter is defined for 2025, however. Charged piston engines are not considered in the current regulation and the applicable reference pressure ratio is not defined. Therefore, the pressure ratio could alternatively be based on the charging pressure ratio (margin -53% with respect to CAEP/6) or the peak pressure ratio (margin -95% w.r.t. CAEP/6). The LEMCOTEC targets of -65% relative to CAEP/2 are met with either interpretation of the applicable pressure ratio as depicted in Figure 7(a).

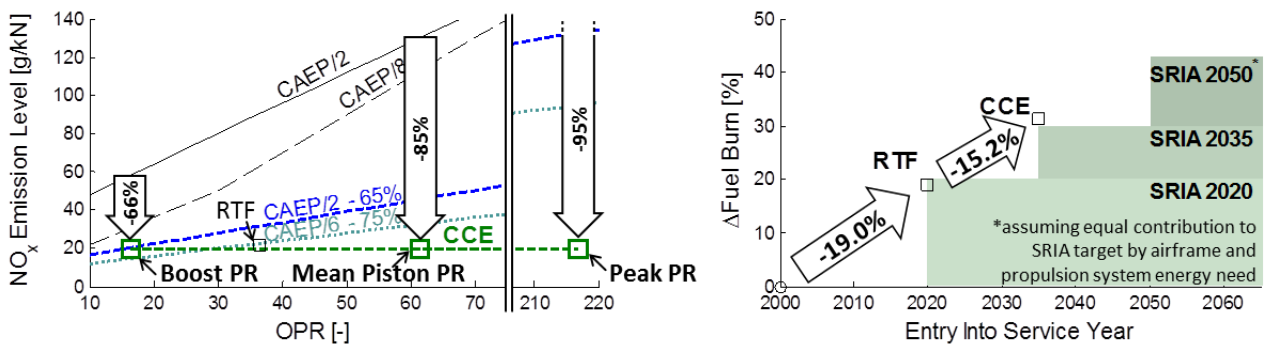

(a) **(b)**

Figure 7. (a) NO_x LTO emissions of the CCE with reference to emission regulations over OPR in contrast to LEMCOTEC target CAEP/2-65% (thick blue dashed line) and NASA N+3 target CAEP/6-75% (teal dotted line). (b) CCE fuel burn reduction potential with reference to emission reduction targets over EIS.

The emission index of the CCE is lower than that of the reference turbofan by virtue of the short residence times at high temperatures and pressures. Another major contributor to the reduction in NO_x emissions is the reduced stoichiometric flame temperature in the Joule/Brayton combustion chamber reduced by up to 500K due to the reduced oxygen content of the piston engine exhaust gas compared to air.

The engine weight was determined according to the approach described in Section III. The estimated piston system weight is 1185 kg (2613lb_m). The nacelle and fan weight remain constant, since fan diameter was kept fixed. The core mass flow in MCL reduces by 28% with respect to the reference. With the approach presented, the IPC weight remains almost constant, HPT weight decreases by 10%, and LPT weight by 50%. On the flipside, combustion chamber weight increases by 74% due to relatively high inlet temperature and low pressure. The HPC is dispensed with. While the turbo machine weight only reduces by 13%, the total engine weight increases by 31% compared to the reference.

The resulting fuel burn savings are 15.2% on the design mission and 16.0% on the 500nm off-design mission as displayed in Table 3. The TSFC improvements are diminished by about 2.5 percent points due to the increase in engine weight. The fuel burn reduction and resulting equivalent reduction of CO_2 emissions compared to the RTF powered aircraft allow for a total reduction of 31.3% with respect to year 2000 from power plant improvements only, i.e. with a Y2000 technology standard airframe. This would allow meeting the SRIA target of -30% energy need from propulsion and power for the year 2035 as depicted in Figure 7(b, prev. page) above. The technology may be combined synergistically with annexed technology such as intercooling, adaptive geometries[43], or boundary layer ingestion[44] to achieve emission reduction targets for Y2050. With the concept and application formulated, but no experimental proof-of-concept, the concept reached Technology Readiness Level (TRL) 2[45].

Table 3. Fuel Burn (FB) deltas for design and 500nm off-design mission based on Exchange Factors (EF).

		Design mission		**500nm mission**	
Parameter	EF unit	EF value	Delta	EF value	Delta
TSFC delta [%]	%FB/1%SFC	1.29	-17.5	1.28	-18.5
Weight delta [kg]	%FB/500kg weight	4.08	+908	4.24	+908
Nacelle diameter delta [“]	%FB/1” diameter	0.18	0	0.15	0
Fuel burn delta [%]			-15.2		-16.0

V. Conclusion

An engine concept for reaching radical improvements in engine efficiency has been introduced, conceptually elaborated and assessed. The engine reaches peak pressure ratios over 300 at Maximum Climb conditions that allow for Thrust Specific Fuel Consumption (TSFC) improvements of 17.5% during cruise on the design mission and a fuel burn saving of 15.2% relative to a regional turbofan platform. On short-haul 500nm missions, the fuel burn saving is even 16.0%. The design philosophy of the engine results in an increase of weight by 31% compared to a turbofan, which is much smaller than for compound engines in the past. Hence, the thrust-to-weight ratio relatively close to a turbofan architecture. The NO_x emissions reduce by about 10% by virtue of short residence times at high temperatures in the piston engine and reduced oxygen content in the combustion chamber. Overall, the engine concept would allow to meet the SRIA emission reduction targets for 2035 for NO_x and CO_2.

The Composite Cycle Engine (CCE) concepts provides an attainable technology step for next generation aeronautical engines that lies on the roadmap towards 2050. When considering additional improvements on component level or the synergistic combination with annexed technology such as intercooling or adaptive geometries, the CCE may allow for reaching or coming close to 2050 efficiency improvement goals.

The study took the concept to Technology Readiness Level (TRL) 2. Since the TRL of the component technologies is very mature, a quick advance in TRL may be expected when advancing the concept definition. Further elaboration of the engine concept will need to address aerodynamic and structural implications of the interaction of piston and turbo components, abnormal operations, scalability, and noise. The preliminary studies indicate that flow pulsation can be reduced to a negligible level with buffering volumes, but a more detailed investigation is necessary. A more detailed conceptualization of the engine components with the resulting engine weight needs to be performed to confirm the fuel savings. Further concepts for the implementation of the piston system such as 4-stroke engines or Wankel-type rotary engines need to be studied to identify the most synergistic combination of piston and turbo engine parts of the CCE.

Acknowledgments

This work is financially supported by the European Commission under the „LEMCOTEC – Low Emissions Core-Engine Technologies”, a Collaborative Project co-funded by the European Commission within the Seventh Framework Programme (2007-2013) under the Grant Agreement n° 283216. The authors would like to thank Oliver Schmitz for his contributions to concept exploration and model development during the first phase of the project. Moreover, gratitude is conveyed to Professor Mirko Hornung, Askin T. Isikveren and Kay O. Plötner for valuable advice.

References

[1] European Commission, *Flightpath 2050: Europe's Vision for Aviation*, Luxembourg, 2011.

[2] Advisory Council for Aviation Research and innovation in Europe (ACARE), *Realising Europe's Vision for Aviation - Strategic Research & Innovation Agenda - Volume 1*, 2012.

[3] Air Transport Action Group (ATAG), "The Right Flightpath to Reduce Aviation Emissions," 2010.

[4] Bradley, M. K., and Droney, C. K., *Subsonic Ultra Green Aircraft Research Phase II : N+4 Advanced Concept Development*, NASA CR-2012-217556, Huntington Beach, California, 2012.

[5] Kurzke, J., "Achieving Maximum Thermal Efficiency with the Simple Gas Turbine Cycle," *Proceedings of Ninth CEAS European Propulsion Forum: Virtual Engine—A Challenge for Integrated Computer Modelling*, 2003.

[6] Benini, E., *Advances in Gas Turbine Technology*, InTech, 2011.

[7] Tennant, D. W. H., and Walsham, B. E., *The Turbocompound Diesel Engine*, SAE Technical Paper 890647, 1989.

[8] Flight Global, "Napier Nomad - An Engine of Outstanding Efficiency," *Flight Global*, Apr. 1954, pp. 543–551.

[9] Wilkinson, P. H., *Aircraft Engines of the World 1966/67*, New York, 1967.

[10] Daly, M., *Jane's Aero Engines 2013/2014*, Jane's Information Group, Coulsdon, UK, 2013.

[11] Soekkha, H. M., *Aviation Safety: Human Factors, System Engineering, Flight Operations, Economics, Strategies & Management*, CRC Press, Rotterdam, 1997.

[12] Ekstrand, C., and Pandey, M., "New ETOPS Regulations," *Boeing Aero*, Apr. 2003, pp. 3–11.

[13] Schulte, D., "Estimating Maintenance Reserves," *Boeing Aero*, Oct. 2013, pp. 4–11.

[14] D. Napier & Son Ltd., "Napier Nomad - The World's Finest Composite Aircraft Engine," *Flight and Aircraft Engineer*, Sep. 1951, p. 9.

[15] Horlock, J. H., *Advanced Gas Turbine Cycles*, Elsevier Science, Oxford, UK, 2003.

[16] Zhao, X., Grönstedt, T., and Kyprianidis, K. G., "Assessment of the Performance Potential for a Two-Pass Cross Flow Intercooler for Aero Engine Applications," *International Society for Airbreathing Engines (ISABE)*, Busan, South Korea, 2013.

[17] Camilleri, W., and Anselmi, E., "Concept Description and Assessment of the Main Features of a Geared Intercooled Reversed Flow Core Engine," *Proceedings of the Institution of Mechanical Engineers, Part G: Journal of Aerospace Engineering*, 2014.

[18] Von der Bank, R., Donnerhack, S., Rae, A., Cazalens, M., Lundbladh, A., and Dietz, M., "LEMCOTEC: Improving the Core-Engine Thermal Efficiency," *ASME Turbo Expo 2014: Turbine Technical Conference and Exposition*, Düsseldorf, Germany, 2014.

[19] Mollenhauer, K., and Tschöke, H., *Handbook of Diesel Engines*, Springer-Verlag, Berlin, 2010.

[20] Merker, G. P., and Teichmann, R., *Grundlagen Verbrennungsmotoren*, Springer Fachmedien, Wiesbaden, 2014.

[21] Kurzke, J., "GasTurb 11 - Design and Off-Design Performance of Gas Turbines," Manual, 2007.

[22] Kurzke, J., “Compressor and Turbine Maps for Gas Turbine Performance Computer Programs - Issue 3,” Manual, 2013.

[23] Kurzke, J., “GasTurb Details 5 - An Utility for GasTurb 11,”, Manual, 2007.

[24] Assanis, D. N., Ekchian, J. E., Frank, R. M., and Heywood, J. B., “A Computer Simulation of the Turbo-charged Turbocompounded Diesel Engine System: A Description of the Thermodynamic and Heat Transfer Models,” NASA CR-174971, Cleveland, Ohio, 1985.

[25] VanGerpen, J. H., “A Two-Stroke Diesel Engine Simulation Program,” NASA CR-185155, Ames, Iowa, 1990.

[26] Hayhurst, A. N., and Vince, I. M., “Nitric Oxide Formation from N2 in Flames: The Importance of ‘Prompt’ NO,” *Progress in Energy and Combustion Science*, Vol. 6, 1980, pp. 35–51.

[27] Kee, R. J., Rupley, F. M., Meeks, E., and Miller, J. A., “Chemkin-III: A FORTRAN Chemical Kinetics Package for the Analysis of Gas-Phase Chemical and Plasma Kinetics,” User Manual, 1996.

[28] Andersson, P., “Models for Predicting the NOx Exhaust Pollutants in a Diesel Engine,” Diploma Paper, Lund University, 1989.

[29] Maiboom, A., Tauzia, X., Hétet, J.-F., Cormerais, M., Tounsi, M., Jaine, T., and Blanchin, S., “Various Effects of EGR on Combustion and Emissions on an Automotive DI Diesel Engine: Numerical and Experimental Study,” SAE Technical Paper 2007-01-1834, 2007.

[30] Weston, K. C., *Energy Conversion*, 2000.

[31] European Aviation Safety Agency (EASA), “ICAO Aircraft Engine Emission Databank (Version 20b),” URL: https://easa.europa.eu/document-library/icao-aircraft-engine-emissions-databank, [last accessed 16 June 2015].

[32] Tacina, R., Wey, C., Laing, P., and Mansour, A., “A Low NOx Lean-Direct Injection, Multipoint Integrated Module Combuster Concept for Advanced Aircraft Gas Turbines,” NASA/TM—2002-211347, 2002.

[33] Joos, F., “Field Experience with the Sequential Combustion System of the GT24/GT26 Gas Turbine Family,” *ABB Review*, 5/1998, pp. 12–20.

[34] Güthe, F., Hellat, J., and Flohr, P., “The Reheat Concept: The Proven Pathway to Ultralow Emissions and High Efficiency and Flexibility,” *Journal of Engineering for Gas Turbines and Power*, vol. 131, 2008, p. 021503.

[35] Köhler, E., and Flierl, R., *Verbrennungsmotoren - Motormechanik, Berechnung und Auslegung des Hubkolbenmotors*, Vieweg+Teubner | GWV Fachverlage GmbH, Wiesbaden, 2009.

[36] Van Basshuysen, R., and Schäfer, F., *Handbuch Verbrennungsmotor*, Vieweg+Teubner | GWV Fachverlage GmbH, Wiesbaden , 2010.

[37] Cevik, M., Rebbert, M., and Maassen, F., “Weight and Friction Optimized Cranktrain Design Supported by Coupled CAE Tools,” *SAE World Congress & Exhibition*, Detroit, Michigan, 2009.

[38] Castor, J., Martin, J., and Bradley, C., “Compound Cycle Engine for Helicopter Application,” NASA CR-180824, Cleveland, Ohio, 1987.

[39] Schaber, R., “Numerische Auslegung und Simulation von Gasturbinen,” Dissertation, Lehrstuhl für Flugantriebe, Institut für Luft- und Raumfahrt, Technische Universität München, 2000.

[40] Grieb, H., *Verdichter für Turbo-Flugtriebwerke*, Springer-Verlag, Berlin, 2009.

[41] Von der Bank, R., Donnerhack, S., Rae, A., Poutriquet, F., Lundbladh, A., and Schweinberger, A., "Technologies for High Thermal Efficiency Aero-Engines," *AVT-230/RSM-033 Specialists Meeting on Advanced Aircraft Propulsion Systems*, Rzeszów, Poland, 2015.

[42] ICAO, *Annex 16 to the Convention on International Civil Aviation - Environmental Protection - Volume II - Aircraft Engine Emissions*, International Civil Aviation Organization , Montréal, Quebec, Canada, 2008.

[43] Da Rocha-Schmidt, L., Hermanutz, A., Baier, H., Seitz, A., Bijewitz, J., Isikveren, A. T., Scarpa, F., Allegri, G., Remillat, C., Feuilloley, E., Majic, F., O'Reilly, C., and Efraimsson, G., "Progress towards Adaptive Aircraft Engine Nacelles," *29th International Congress of the Aeronautical Sciences*, St Petersburg, Russia, 2014.

[44] Seitz, A., Bijewitz, J., Kaiser, S., and Wortmann, G., "Conceptual Investigation of a Propulsive Fuselage Aircraft Layout," *Aircraft Engineering and Aerospace Technology Journal*, vol. 86, 2014, pp. 464–472.

[45] National Aeronautics and Space Administration (NASA), "NASA Systems Engineering Handbook," NASA/SP-2007-6105, Washington, D.C, 2007.